CHEMISTRY OF MATERIALS

Communication

pubs.acs.org/cm

# Droplet Manipulation on Wettable Gradient Surfaces with Micro-/Nano-Hierarchical Structure

Yong P. Hou,[‡] Shi L. Feng,[‡] Li M. Dai,[*,§] and Yong M. Zheng[*,‡]

[‡]Key Laboratory of Bio-Inspired Smart Interfacial Science and Technology of Ministry of Education, School of Chemistry and Environment, Beihang University, Beijing, 100191, People's Republic of China

[§]Center of Advanced Science and Engineering for Carbon, Department of Macromolecular Science and Engineering, Case Western Reserve University, Cleveland, Ohio 44106, United States

Supporting Information

The materials with an ability to control the movement of droplet via wettable gradient surface have attracted significant interest as they hold promising applications in microfluidics,[1] chemical sensors,[2] biomolecular interactions[3] and electro-analytical chemistry.[4] Various techniques have been used to fabricate the wettable gradient via gradients of chemical composition, physical structure, or both.[5] For instance, Chaudhury and Whitesides[6] generated a chemical composition gradient on the surface of a polished silicon wafer by diffusing deposition of decyltrichlorosilane vapor. Whereas Shastry et al.[7] fabricated a roughness gradient by controlling the surface microscale structure to form the wettable gradient on a silicon substrate. In fact, to realize self-propelled motion of droplets on a wettable gradient surface, the contact angle hysteresis (CAH, i.e., the difference between the advanced (ACA) and receding contact angles (RCA)) should be lower than 10°.[6] As reported,[8,9] even on a large wettable gradient surface, a water droplet only exhibits directional spreading behavior due to high hysteresis force. The fabrication of micro/nano-hierarchical structure is one of fantastic methods to mitigate hysteresis force. To date, many fabrication methods have been proposed to prepare micro/nano-hierarchical structure.[7,8] However, many of these fabrication processes involve sophisticated multisteps and fluorination treatment, which are often time-consuming and harmful to the environment. It remains a great challenge to generate wettable gradient surfaces with micro/nano-hierarchical structure via a simple, rapid and environment-friendly process to achieve the control of the movement behavior of droplet. In this study, we realize controlled self-propelled motion of droplets by simply improved one-step electrodeposition method. The results indicate that, during deposition process, not only could the wettable gradient be formed via the cooperation of surface geometrical structure gradient and chemical composition gradient, but micro/nano-hierarchical structure is prepared by depositing nano copper particles on the surface of stainless steel mesh. Accordingly, various wettable gradient surfaces with low CAH could be fabricated easily. On such surfaces, not only a droplet could move along given direction but also two droplets move away from one another. More importantly, the movement distance could be precisely predicted by the force analysis and controlled by the initial position of the droplet and/or the magnitude of the wettable gradient, which should have important implications to both fundamental research and practical applications, ranging from smart materials through microfluidics to biomedical devices.[10−12]

Micro/nanohierarchical structure plays an important role in regulating the surface wettability and mitigating hysteresis force.[11] Many complex processes have been used to form the hierarchical structure.[13,14] The electrochemical method is considered to be one of the most promising techniques to produce nanostructure over large areas. It has some advantages, including low cost, facile and rapid fabrication and easy scale-up. Here, we took advantage of stainless steel mesh features (micro pore) to form micro/nano-hierarchical surface via cathodic electrodeposition method (Figure 1, see the Supporting Information for description of the experiment). A narrow-strip copper plate was used as an anode to form a current gradient ($I_3 > I_2 > I_1$) (the resistance of the electrolyte is proportional to the distance between the anode and cathode)

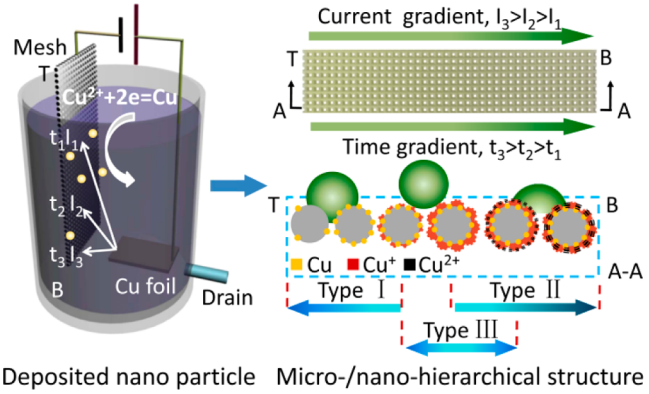


**Figure 1.** Schematic illustration of the formation of various wettable gradient surfaces with micro/nano-hierarchical structure via one-step cathodic deposition method by depositing nano copper particles on the surface of stainless steel mesh. A narrow-strip copper plate was used as an anode to form a current gradient ($I_3 > I_2 > I_1$) and a drain was used to adjust the deposition time ($t_3 > t_2 > t_1$). By this way, the gradients of chemical composition and physical structure are formed. By adjusting the electrodeposition condition, various wettable gradient surfaces with micro/nano-hierarchical structure could be fabricated easily.

Received: April 17, 2016
Revised: May 18, 2016
Published: May 20, 2016





DOI: 10.1021/acs.chemmater.6b01544
Chem. Mater. 2016, 28, 3625−3629

and a drain was used to adjust the deposition time to form a time gradient ($t_3 > t_2 > t_1$). By combining the effect of current gradient and time gradient, the change of the surface geometrical structure and chemical composition could be controlled and various wettable gradients could be fabricated easily via adjusting the deposition condition, i.e., voltage ($V$) and flow velocity of electrolyte ($f$).

It is well-known that the surface wettability of surface is determined by the topographic structure and the surface chemical composition. The Cassie−Baxter eq (eq 1) is one of the models that describes the behavior of a droplet on a rough solid surface:[15−18]

$$\cos\theta = f_{s1}(1 + \cos\theta_0) - 1 \quad (1)$$

in which $\theta$ is the apparent contact angles (CAs) on a rough surface, $\theta_0$ is the intrinsic CAs on a flat surface, $f_{s1}$ is the fraction of the solid/water interface. Figure 2 describes the change of surface microstructure and wettability of three samples (see Figures S1 and S2 of the Supporting Information for details). The results of scanning electron microscopy (SEM) indicate that, after electrodeposition, copper microclusters are deposited on every wire, but the pores of the mesh remain clear. For Sample-A ($V$ = 3 V, $f$ = 3.5 L/h), at the top area of stainless steel mesh, both the current density and deposition time are relatively small and only some occasional spherical papillae with an average length of 0.5−1 $\mu$m, distribute sparsely over the surface (Figure 2a1). Along the direction from T to B (T: top area and B: bottom area of the stainless steel mesh during the perpendicularly electrodeposition), with increasing deposition time, spherical papillae become larger and then grow into bigger ones (Figure 2a2,a3,a4,a5). Hence, the value of $f_{s1}$ decreases, leading to an increase in the surface roughness and hydrophobicity (eq 1). In addition, when the reaction time increases up to 40 s, the X-ray diffraction (XRD) results show that some of the copper components are oxidized to form cuprous oxide ($Cu_2O$) (Figure S3a). Considering the standard electrode potential of Cu (+0.34 V), Cu can be easily oxidized.[19] Because of the hydrophobicity of $Cu_2O$,[20] more air is trapped between the particles and the value of $f_{s1}$ further reduces, leading to superhydrophobicity on the bottom area (163°). Therefore, the corresponding CAs increase from 128° to 163° gradually and the wettable gradient reaches 2.92°/mm.

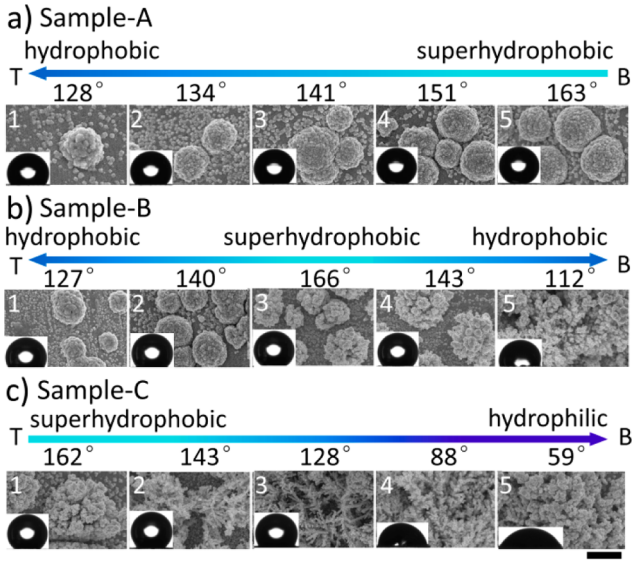


**Figure 2.** Change of surface microstructure and corresponding wettability on different areas of different samples. (a) Sample-A ($V$ = 3 V, $f$ = 3.5 L/h). Along the direction from T to B, spherical papillae are getting larger and the corresponding CAs increase from 128° to 163° gradually and the wettable gradient reaches 2.92°/mm. (b) Sample-B ($V$ = 4 V, $f$ = 3.5 L/h). From T to B, the dense papillae change to the cauliflower-shaped structure and then the cauliflower-shaped structure grows up to connect together. CAs change from 127° to 166° and then decrease to 112°, showing an upside-down V-shape wettable gradient of 7.67°/mm. (c) Sample-C ($V$ = 5 V, $f$ = 3.5 L/h). Because of the fast deposition velocity, from T to B, the cauliflower-shaped structure changes to coral-like structure. The corresponding CAs decrease from 162° to 59°, showing a wettable gradient of 5.18°/mm. The volume of droplets is 5 $\mu$L and the scale bar is 1 $\mu$m (T: top area and B: bottom area of the stainless steel mesh during the perpendicularly cathodic electrodeposition process).

An increase in potential helps the deposition particles to grow larger and produce extended metal nanostructure.[19] When the voltage becomes 4 V ($f$ = 3.5 L/h, Sample-B), more spherical papillae are observed on the top area within a shorter period (Figure 2b1,b2). From T to B, the dense papillae change into the cauliflower-shaped structure on the middle area, i.e., bihierarchical structure changes to trihierarchical structure (Figure 2b3,b4). Meanwhile, hydrophobic $Cu_2O$ also appears on the surface (Figure S3b). Consequently, the middle part of Sample-B exhibits superhydrophobicity (166°). Thereafter, the cauliflower-shaped structure grows up to connect together (Figure 2b5) and the roughness reduces gradually ($f_{s1}$ increases), leading to gradually decreased CAs (according to Equ. 1). Interestingly, we also observed that the color of stainless steel mesh changed from yellow to black on the bottom of the mesh (under deposition condition of 4 V, 40 s). We used high-resolution X-ray photoelectron spectroscopy (XPS) spectra to check the chemical composition (Figure S4). The most important character is the shakeup satellite, indicating the presence of hydrophilic cupric oxide (CuO), probably resulting from oxidation reaction between the copper and oxygen in the electrolyte.[19−21] Accordingly, an upside-down V-shape wettable gradient of 7.67°/mm is observed on the Sample-B (CAs change from 127° to 166° and then decrease to 112°).

When the voltage increases to 5 V (3.5 L/h, Sample-C), the driving force for crystallization is amplified further. The SEM results show a large number of isolated cauliflower structure with an average diameter of ~1 $\mu$m uniformly distribute on the top area of mesh (Figure 2c1). From T to B, the surface changes to coralloid clusters (Figure 2c2,c3) and finally, the coralloid clusters grow much bigger, become continuous, and completely cover the surface of the stainless steel wires, forming a nanoporous structure (Figure 2c4,c5). The change of structure induces a decrease in the surface roughness ($f_{s1}$ increases), resulting in the decrease of CAs (according to eq 1). Finally, hydrophilic CuO forms on the bottom part of mesh (Figure S4), and the contact model changes from Cassie state to Wenzel state. The corresponding CAs decrease from 162° to 59°, showing a wettable gradient of 8.58°/mm (Figure 2c). Therefore, the change of CAs for three samples is due to the combined effect of the gradient structure and chemical composition. The current and treatment time could be adjusted by the distance between anode and cathode or flow velocity of electrolyte (Figure S5) and we clarify the relationship between voltage, flow velocity and wettable gradient (Figure S6). The results indicate that various wettable gradient surfaces could be


DOI: 10.1021/acs.chemmater.6b01544
Chem. Mater. 2016, 28, 3625−3629

formed and the magnitude of wettable gradient could be controlled between 1.14 and 8.58°/mm easily by a one-step deposition method.

Figure 3 shows the directional movement of droplets on different sample surfaces. All of droplets show the directional

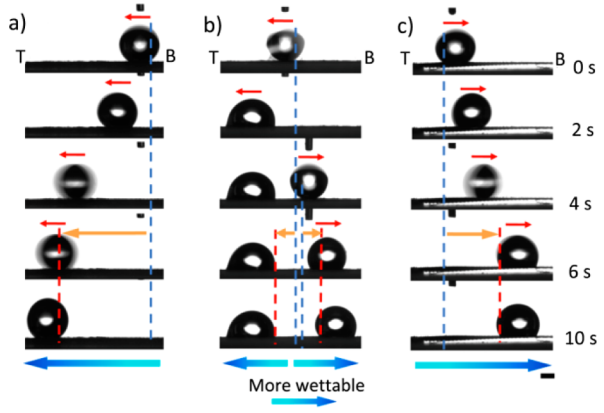


**Figure 3.** Movement behavior of droplet on different sample surfaces. (a) On Sample-A surface. The droplet performs directional motion along direction from B to T. (b) On Sample-B surface. Two droplets move away from one another from the center to two sides (T or B). (c) On Sample-C surface. The droplet shows directional motion along direction from T to B. (T: top area and B: bottom area of the stainless steel mesh during the perpendicularly cathodic electrodeposition process). The volume is 10 $\mu$L and the scale bar is 1 mm.

motion along the wettable gradient direction. For Sample-A (Figure 3a), a droplet performs directional motion along direction from B to T. As for Sample-B, it has an inverse-V-shaped wettable gradient (Figure 3b), thus two droplets move away from one another from the center to two sides. On the surface of Sample-C, the droplet moves along direction from T to B (Figure 3c). Figure S7 shows the change in CAH of the three samples. Along the direction from T to B, for the Sample-A, the CAH decreases continually from 46° to 4°. For Sample-B, the CAH initially decreases from 44° to 3° and then increases to 49°, showing a minimum value on the middle area of mesh. For Sample-C, the value increases from 3° to 84°. Obviously, the CAH has an opposite change trend to that of the CAs. Therefore, when droplets move along the wettable gradient, the CAH increases gradually and droplets would stop finally. Clearly, the electrodeposition-induced gradient surfaces realize directional motion of droplet.

We further performed a set of experiments to investigate the motion behavior of droplets by measuring the movement distance of the droplet ($L_s$) from different initial positions ($L_i$) (the zero position is defined as the boundary between treated part and untreated part) on the surfaces of Sample-A and Sample-C (for Sample-B, as the movement distance is very short, this experiment is not investigated on it). As shown in Figure 4a–c, for Sample-C, when a droplet is dripped within 10 mm away from the top end of the stainless steel mesh, the droplet would exhibit self-propelled motion and it would always stop and be balanced at the same position ($x$) no matter where it is released, i.e., $x = L_s + L_i$ = constant =10.1 mm. In other regions, no movement behavior appears and the droplets only spread along the wettable gradient, exhibiting an asymmetric shape (Figure 4d). A similar movement behavior is also observed on the surface of Sample-A and the equilibrium position changes to 6.7 mm. Therefore, for a given wettable

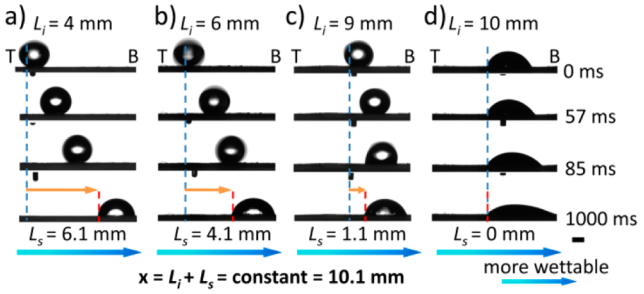


**Figure 4.** Movement behavior of droplets on the Sample-C surface. The as-observed time can be in 1000 ms. (a) The initial position ($L_i$), $L_i$ = 4.0 mm, the movement distance of droplet ($L_s$), $L_s$ = 6.1 mm. (b) $L_i$ = 6.0 mm, $L_s$ = 4.1 mm. (c) $L_i$ = 9.0 mm, $L_s$ = 1.1 mm. (d) $L_i$ = 10.0 mm, $L_s$ = 0 mm (the zero position is defined as the boundary between treated part and untreated part). The volume of droplet is 10 $\mu$L and the scale bar is 1 mm. The results indicate that a droplet would always stop and be balanced at the same position ($L_i$ + $L_s$ = 10.1 mm) no matter where it is released when a droplet is dripped within 10 mm away to top end of stainless steel mesh. Otherwise, droplets would only spread along the wettable gradient, exhibiting an asymmetric shape (T: top area and B: bottom area of the stainless steel mesh during the perpendicularly cathodic electrodeposition process).

gradient surface, there seem to be an equilibrium position and droplets would always stop and be balanced at the same position.

To gain better understanding of the unique phenomenon, we analyze the forces exerted on the droplets,[6] i.e., the wettable gradient force ($F_w$) and the hysteresis force ($F_H$), which result from wettable gradient and contact angle hysteresis, respectively (it is also important to mention here that the effect of gravity and inertial forces could be neglected for a droplet of volume 10 mL[12]). The $F_w$ (details of explanation shown in Figure S8) drives water droplet toward the more wettable region of surface, which is described as[6]

$$F_w = \pi\gamma R^2 k \sin\theta \quad (2)$$

where $R$ is the base radius of the droplet, $\gamma$ is the surface tension of water, $k$ is the wettable gradient and $\theta$ is the position-responsive sessile CA of the droplet. The $F_H$, opposite to the moving direction, is described as[8]

$$F_H = 2\gamma R(\cos\theta_{ro} - \cos\theta_{ao}) \quad (3)$$

where $\theta_{ro}$ and $\theta_{ao}$ are the position-dependent receding and advancing CAs at the central line of the drop on the solid surface, respectively. When droplets (10 $\mu$L) are dripped within equilibrium position, the radius could be seemed as a constant ($R \sim 1.5$ mm). According to Figures S6 and S7, we found for the three samples there is a linear relationship among CA and ACA, RCA (Figure 5a), i.e., $y_{(ACA)} = 0.6x_{(CA)} + 54$ and $y_{(RCA)} = 1.5x_{(CA)} - 81$, where $x_{(CA)}$, $y_{(ACA)}$ and $y_{(RCA)}$ are CA, ACA and RCA, respectively. Therefore, the total force $F_T$ ($F_T(\theta, k) = F_w - F_H$) could be regarded as a function of contact angle ($\theta$) and wettable gradient ($k$),

$$F_T = \pi\gamma R^2 k \sin\theta - 2\gamma R[\cos(1.5\theta - 81) - \cos(0.6\theta + 54)]$$

Therefore, we could get the values of $F_T$ at different conditions (Figure 5b). For a given surface ($k$ = constant), the $F_T$ is a function of $\theta$. If the $F_T > 0$, droplet would exhibit self-propelled motion along the direction of wettable gradient



DOI: 10.1021/acs.chemmater.6b01544
Chem. Mater. 2016, 28, 3625–3629

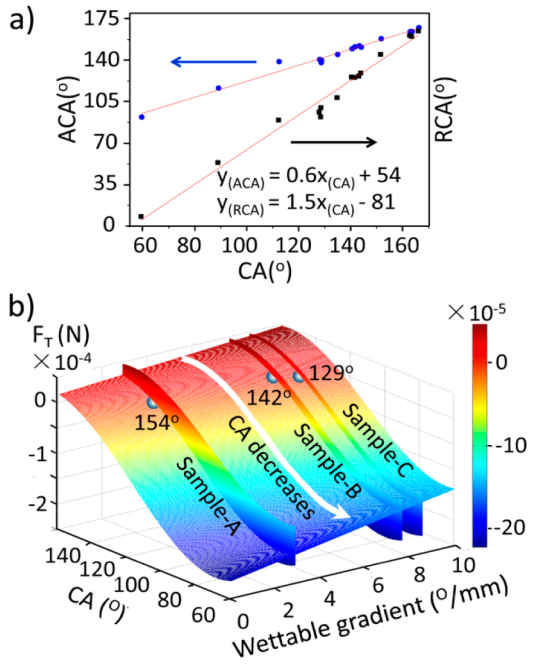


**Figure 5.** (a) Fitted linear relationship of contact angle (CA) versus advancing contact angle (ACA) and receding contact angle (RCA): $y_{(ACA)} = 0.6x_{(CA)} + 54$ and $y_{(RCA)} = 1.5x_{(CA)} - 81$, where $x_{(CA)}$, $y_{(ACA)}$ and $y_{(RCA)}$ are CA, ACA and RCA, respectively. (b) Calculated total ($F_T$) at different positions (different CA and wettable gradient). The equilibrium contact angles for Sample-A, Sample-B and Sample-C ($F_T$ = 0) are 154°, 142° and 129°, respectively.

(denoted by the direction of the arrow Figure 5b). During the movement process, the $F_T$ decreases gradually. When the $F_T$ = 0, the droplet would stop. Therefore, for a given wettable gradient surface, droplets would always stop and be balanced at the same position (the point $F_T$ ($\theta$) = 0). More interestingly, from Figure 5b, we could get the equilibrium CA for different conditions ($\theta$, $k$) to predict the movement behavior of droplet. For example, we obtain the equilibrium contact angles for Sample-A ($k$ = 2.92°/mm), Sample-B ($k$ = 7.67°/mm) and Sample-C ($k$ = 8.58°/mm) are 154°, 142° and 129°, respectively. Then, according to Figure S6b, we could deduce that the equilibrium position for Sample-A, Sample-B and Sample-C are 6.4, 3.0 and 9.9 mm, in good agreement with our observations (actual equilibrium positions for Sample-A, Sample-B and Sample-C are 6.7, 2.9 and 10.1 mm). Accordingly, the result implies that movement behavior of droplet could be predicted from the values of CA and the wettability gradient (according to Figure 5b) and the movement distance could be controlled by adjusting the initial position and/or the magnitude of the wettable gradient.

In summary, we have developed a one-step gradient electrodeposition method for preparing a novel functional mesh film with micro/nano-hierarchical structure, large wettable gradient and low CAH. The direction and value of wettable gradient could be adjusted easily via electrodeposition condition. On such surfaces, not only a droplet could move along given direction but also two droplets move away from one another. More importantly, the movement distance could be precisely predicted by the force analysis and controlled by the initial position of the droplet and/or the magnitude of the wettable gradient. This method can be applied on many conductive substrates (copper, aluminum, etc.) to fabricate variously shaped wettable gradients for potential applications in microfluidics, smart devices and biomaterials and so on.[9]

## ■ ASSOCIATED CONTENT

### Supporting Information

The Supporting Information is available free of charge on the ACS Publications website at DOI: 10.1021/acs.chemmater.6b01544.

Experimental details, surface wettability, microstructure and chemical composition of different areas prepared at different deposition conditions (PDF).

## ■ AUTHOR INFORMATION


### Corresponding Authors

*Yong M. Zheng, E-mail: zhengym@buaa.edu.cn.
*Li M. Dai, E-mail: liming.dai@case.edu.


### Notes

The authors declare no competing financial interest.

## ■ ACKNOWLEDGMENTS


This work was supported by National Key Basic Research Program of China (2013CB933001), National Natural Science Foundation of China (21234001, 51203006, 21473007), Fundamental Research Funds for Central Universities (YWF-15-HHXY-017, YWF-16-JCTD-A-01) and Aeronautical Science Foundation of China (2015ZF51060). L.D. is grateful to National Science Foundation for financial support (NSF-CMMI-1266295)


## ■ REFERENCES


(1) Zhang, G.; Zhang, X.; Li, M.; Su, Z. A surface with superoleophilic-to-superoleophobic wettability gradient. *ACS Appl. Mater. Interfaces* **2014**, *6*, 1729−1733.
(2) Yu, X.; Wang, Z.; Jiang, Y.; Zhang, X. Surface Gradient Material: From Superhydrophobicity to Superhydrophilicity. *Langmuir* **2006**, *22*, 4483−4486.
(3) Jeong, B. J.; Lee, J. H.; Lee, H. B. Preparation and Characterization of Comb-like PEO Gradient Surfaces. *J. Colloid Interface Sci.* **1996**, *178*, 757−763.
(4) Wang, L.; Peng, B.; Su, Z. Tunable wettability and rewritable wettability gradient from superhydrophilicity to superhydrophobicity. *Langmuir* **2010**, *26*, 12203−12208.
(5) Sun, C.; Zhao, X. W.; Han, Y. H.; Gu, Z. Z. Control of water droplet motion by alteration of roughness gradient on silicon wafer by laser surface treatment. *Thin Solid Films* **2008**, *516*, 4059−4063.
(6) Chaudhury, M. K.; Whitesides, G. M. How to Make Water Run Uphill. *Science* **1992**, *256*, 1539−1541.
(7) Shastry, A.; Case, M. J.; Böhringer, K. F. Directing Droplets Using Microstructured Surfaces. *Langmuir* **2006**, *22*, 6161−6167.
(8) Feng, S.; Wang, S.; Liu, C.; Zheng, Y.; Hou, Y. Controlled droplet transport on a gradient adhesion surface. *Chem. Commun.* **2015**, *51*, 6010−6013.
(9) Feng, S.; Wang, S.; Gao, L.; Li, G.; Hou, Y.; Zheng, Y. Controlled directional water-droplet spreading on a high-adhesion surface. *Angew. Chem., Int. Ed.* **2014**, *53*, 6163−6167.
(10) Yang, D.; Piech, M.; Bell, N. S.; Gust, D.; Vail, S.; Garcia, A. A.; Schneider, J.; Park, C. D.; Hayes, M. A.; Picraux, S. T. Photon Control of Liquid Motion on Reversibly Photoresponsive Surfaces. *Langmuir* **2007**, *23*, 10864−10872.
(11) Hou, Y.; Xue, B.; Guan, S.; Feng, S.; Geng, Z.; Sui, X.; Lu, J.; Gao, L.; Jiang, L. Temperature-controlled directional spreading of water on a surface with high hysteresis. *NPG Asia Mater.* **2013**, *5*, e77.
(12) Karapetsas, G.; Sahu, K. C.; Sefiane, K.; Matar, O. K. Thermocapillary-driven motion of a sessile drop: effect of non-



DOI: 10.1021/acs.chemmater.6b01544
*Chem. Mater.* 2016, 28, 3625−3629

monotonic dependence of surface tension on temperature. *Langmuir* **2014**, *30*, 4310−4321.
(13) Greiner, C.; Arzt, E.; del Campo, A. Hierarchical Gecko-Like Adhesives. *Adv. Mater.* **2009**, *21*, 479−482.
(14) Jokinen, V.; Sainiemi, L.; Franssila, S. Complex Droplets on Chemically Modified Silicon Nanograss. *Adv. Mater.* **2008**, *20*, 3453−3456.
(15) Sung, M. M.; Sung, K.; Kim, C. G.; Lee, S. S.; Kim, Y. Self-Assembled Monolayers of Alkanethiols on Oxidized Copper Surfaces. *J. Phys. Chem. B* **2000**, *104*, 2273−2277.
(16) Wang, S.; Song, Y.; Jiang, L. Microscale and nanoscale hierarchical structured mesh films with superhydrophobic and superoleophilic properties induced by long-chain fatty acids. *Nanotechnology* **2007**, *18*, 015103.
(17) Shin, H. C.; Dong, J.; Liu, M. Nanoporous Structures Prepared by an Electrochemical Deposition Process. *Adv. Mater.* **2003**, *15*, 1610−1614.
(18) Cassie, A. B. D; Baxter, S. Wettability of porous surfaces. *Trans. Faraday Soc.* **1944**, *40*, 546−551.
(19) Wang, G.; Zhang, T. Y. Easy route to the wettability cycling of copper surface between superhydrophobicity and superhydrophilicity. *ACS Appl. Mater. Interfaces* **2012**, *4*, 273−279.
(20) Ding, Y.; Li, Y.; Yang, L.; Li, Z.; Xin, W.; Liu, X.; Pan, L.; Zhao, J. The fabrication of controlled coral-like Cu2O films and their hydrophobic property. *Appl. Surf. Sci.* **2013**, *266*, 395−399.
(21) Najmeh, D.; Paria, S.; Abolfazl, K. Self-Movement of Water Droplet at the Gradient Nanostructure of Cu Fabricated Using Bipolar Electrochemistry. *Langmuir* **2014**, *30*, 1376−1382.



DOI: 10.1021/acs.chemmater.6b01544
*Chem. Mater.* 2016, 28, 3625−3629